SIMULATION OF INTEGRATED BEAM EXPERIMENT DESIGNS*

D. P. Grote and W. M. Sharp

Lawrence Berkeley National Laboratory

1 Cyclotron Road, Bldg 47R0112, Berkeley, CA, 94720-8201

dpgrote@lbl.gov and

510-495-2961

Abstract

Simulation of designs of an Integrated Beam Experiment (IBX) class accelerator have been carried out. These simulations are an important tool for validating such designs. Issues such as envelope mismatch and emittance growth can be examined in a self-consistent manner, including the details of injection, accelerator transitions, long-term transport, and longitudinal compression. The simulations are three-dimensional and time-dependent, and begin at the source. They continue up through the end of the acceleration region, at which point the data is passed on to a separate simulation of the drift compression. Results are be presented.

* This work performed under the auspices of the U.S Department of Energy by University of California, Lawrence Livermore and Lawrence Berkeley National Laboratories under contracts No. W-7405-Eng-48 and DE-AC03-76SF00098.

Introduction

In high current, low emittance beams, that are also nearly collisionless, correlations in the distribution function persist for many betatron wavelengths, making the dynamics sensitive to the initial conditions and to perturbations during transport. For a numerical simulation to have predictive value, therefore, it is essential to model the initial distribution accurately and to follow the same simulation particles throughout the accelerator, thereby maintaining all correlations in the distribution. Since the beam distribution is best known at the source, it is preferable to begin a self-consistent simulation there. Such simulations are challenging due to the length and complexity of a typical accelerators, as well as to the number of particles and fine resolution required to model accurately the six-dimensional beam phase space.

In this paper, numerical simulations are presented of a high current accelerator, from the source to the end of the accelerator. The system modeled here is the Integrated Beam Experiment (IBX), a projected facility currently being developed in concept for construction at Lawrence Berkeley National Laboratory.[2] These simulations are carried out with the computer code Warp [1], which uses the particle-in-cell method to represent the beam and calculates the electrostatic self-field of the beam by solving Poisson's equation. The beam self-magnetic field is unimportant for the parameters used here.

The first section of this paper discusses the illustrative IBX design in detail, giving its layout and parameters, and reviewing the algorithms used for injecting, matching, and controlling the beam. The following section covers the principal results of the simulations. Conclusions and future work are then discussed in the final section.

I. INTEGRATED BEAM EXPERIMENT

The Integrated Beam Experiment (IBX) will explore key physics issues of the high-current heavy-ion beams required for inertial-fusion-energy applications, as well as for high-energy-density plasma science. Scientific research on IBX will provide new insight into the behavior

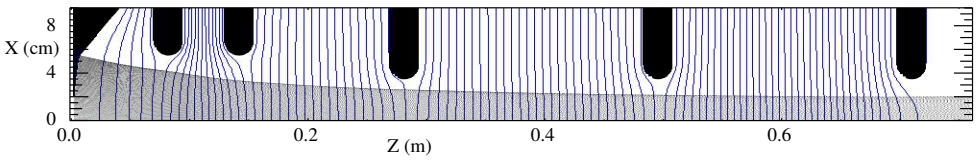

Figure 1: Layout of Pierce column injector. The blue curves show equipotential lines.

of high-current beams, which are non-neutral plasmas with sufficient space charge to exhibit collective effects, including longitudinal space-charge waves, halo formation, and electron-cloud phenomena.

Many IBX parameters are close to values required for a heavy-ion fusion power plant, though the final particle energy and total beam energy will be substantially less. The basic parameters, given in Table I. In this design, the transverse focusing is produced by a periodic FODO lattice with the same field gradient in each of the 44 half-lattice periods (HLPs). The "zeroth-order" parameters [3] result from assuming that the necessary head-to-tail velocity gradient, or "tilt", is applied in the first acceleration gap, and that the beam is accelerated uniformly over the length of the lattice, rather than in discrete gaps. An injector of the Pierce-column type and an electrostatic matching section are used. The simulations here focus on an acceleration scenario with constant beam bunch length during acceleration. The various time-dependent waveforms that are required for the simulation and how they are generated are described below.

A. Injection and matching section

The injector is a conventional Pierce-column design, consisting of a diode followed by a series of biased aperture plates that act as Einzel lenses to provide transverse focusing of the beam. The layout is shown in Fig. 1. Axisymmetric simulations of the injector give a normalized emittance of approximately 0.5 π-mm-mrad, well within acceptable limits. A sizable hook in the radial phase-space distribution is seen at the outer edge, but is a numerical artifact, resulting primarily from poor resolution of the beam edge. In future work, adaptive-mesh-refinement techniques will be incorporated to resolve the issue.[4]

Table I: Basic parameters of the accelerating section for a scenario with constant bunch length.

	Initial	Final
Energy (MeV)	1.71	6.1
Undepressed tune (degrees)	72.	37.
Pulse duration (ns)	200.	107.
Beam end length (ns)	50.	50.
Bunch length (m)	0.58	0.58
Current (A)	0.364	0.682
Line charge (μC/m)	0.125	0.125
Beam radius (cm)	1.07	1.07
Pipe radius (cm)	2.73	2.73
HLP length (m)	0.23	0.23
Quad length (m)	0.127	0.127
Quad field gradient (T/m)	69.5	69.5
Accelerating voltage per HLP (kV)	99.0	99.0

The diode voltage is adjusted to give a constant current density during the beam pulse. The voltage difference across a short virtual region in front of the emitting surface is determined, given the current density, by assuming space-charge-limited emission. As the beam is emitted, the potential in the virtual region rises due to the beam space charge, and so the diode voltage is increased as needed to maintain the voltage difference.[5] The waveform is shown in Fig. 2. The shape of the waveform at early time is not physical but is dependent on the resolution at the source. This non-physicality does not compromise the simulation here, since the current profile is much the same as that produced both with greater refinement and with the ideal waveform. The falloff is somewhat arbitrary and is taken to be the time reversed rise with the time scale halved with a linear falloff at the end so injection is completely cutoff.

The matching section consists of six electric quadrupoles that match the beam from the injector

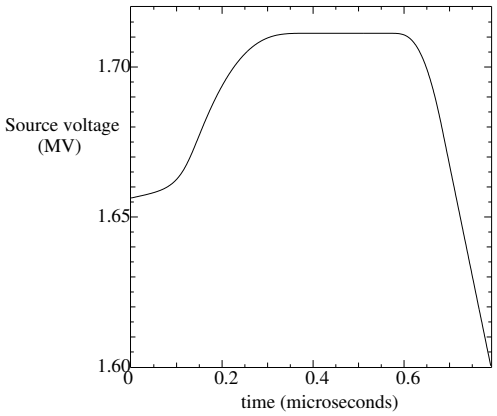

Figure 2: Voltage profile on source.

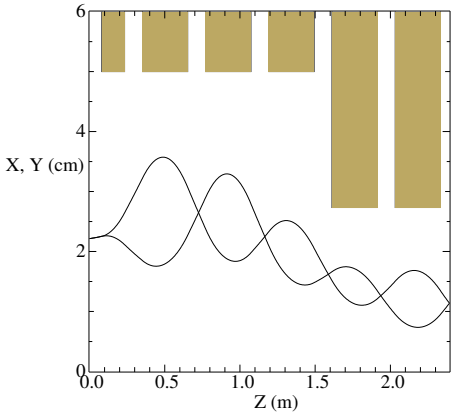

Figure 3: The envelope solution in the matching section. The blocks show the longitudinal extent and transverse aperture of the quadrupoles.

to the accelerating lattice. The matching section developed is shown in Figure 3.

As the beam emerges from the matching section, the waveform applied by the first accelerating gap corrects the axial velocity, removing the effects of space-charge blow-off. The "catching" waveform is calculated dynamically as the beam passes the gap from an average of the energy of particles within the gap.

B. Acceleration and ears

A beam that is accelerated with a constant bunch length will have a velocity tilt, $v_z(t)$, at a given z. Since the beam emerging from the source has a constant v_z, triangular waveforms must be applied to generate the tilt. The waveforms are obtained assuming self-similarity of the bunch as it passes each gap. Most of the tilt is applied in the first gap. All subsequent gaps have a nearly constant voltage near the nominal 99-kV value given in Table I.

As part of the waveform for each gap, an axially confining ear field must be applied to prevent blow-off of the beam ends from space-charge. The waveforms are calculated dynamically as the beam passes each gap. The longitudinal self field along the beam is accumulated between gaps, and the ear waveform is the negative of that, scaled by the ratio of the distance between gaps and the gap length.

II. SIMULATION RESULTS AND DISCUSSION

The basic numerical parameters in the simulations are a mesh of 64x64x768 and 55,000 particles, with a time step of 1 nanosecond. Multiple cases were run with differing resolution to check on convergence. The simulation begins with the field grid fixed in space until the full beam is injected, and then the grid then moves with the beam. Figures 4 and 5 at 1.0 μs show the complete beam part of the way into the matching section. Figures 4 and 5 at 1.5 μs show the beam just as it is passing the first gap where the energy is corrected, as can be seen as the downward step in velocity at the head of the beam. Once the beam enters the transport section, the bulk of the beam is accelerated, leaving the extra tail behind. This can be seen in Figs. 6 and 7 at 2.0 μs. The contours of constant potential show a necking at the point where the tail of the beam begins to separate. The beam is then accelerated through the remainder of the transport section. Figures 6 and 7 at 4.0 μs show the beam near the end of the accelerator. The long thin tail results from particles that are accelerated by the end of the accelerating pulse but are not confined by the ear fields. These particles are primarily remnants of the extra tail that are straggling behind but not completely lost.

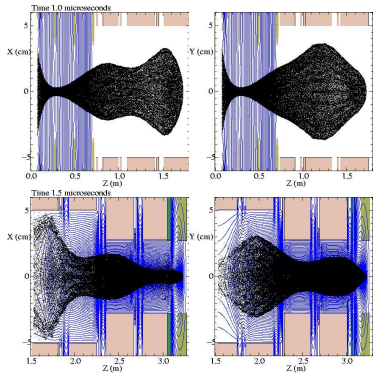

Figure 4: Snapshots of the beam, with equipotential lines overlaid. The blocks along the top and bottom edges show the aperture plates in the injector and the quadrupole rods and end plates.

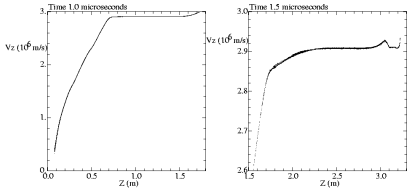

Figure 5: Snapshots of the longitudinal phase space

Once the beam starts its acceleration, it is fairly quiescent. Almost no space-charge waves are launched from the manipulations. This can be seen in Fig. 8 which shows overlays of the line-charge as the beam propagates through the system. The beam also experiences little emittance growth.

The halo that can be seen in the Figure 6 is a good example of the importance of preserving correlations in the distribution. A hook that appears in the radial phase-space of the beam from poor resolution of the source. This correlation created at the source persists through the various beam manipulations, and the particles in the hook become the primary constituent of the halo.

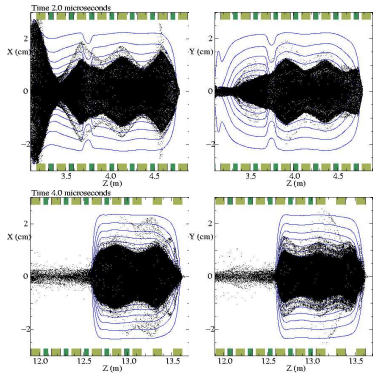

Figure 6: Snapshots of the beam at two later times, with equipotential lines overlaid. The longer blocks at the top and bottom edges indicate the longitudinal extent of the magnetic quadrupole field, while the shorter blocks show the extent of the acceleration gaps.

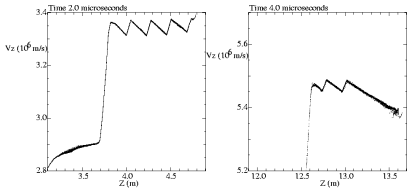

Figure 7: Longitudinal phase-space views at later times.

III. CONCLUSIONS AND FUTURE WORK

Complete simulations of an illustrative IBX design has been carried out, from the source to the end of drift compression. The simulations follow the same particles through all manipulations, thereby maintaining a realistic beam distribution, with all internal correlations, through the accelerator. This type of simulation represents a new modeling capability for high-current ion beams. The simulation results are largely encouraging. The beam can be "caught" as it emerges from the

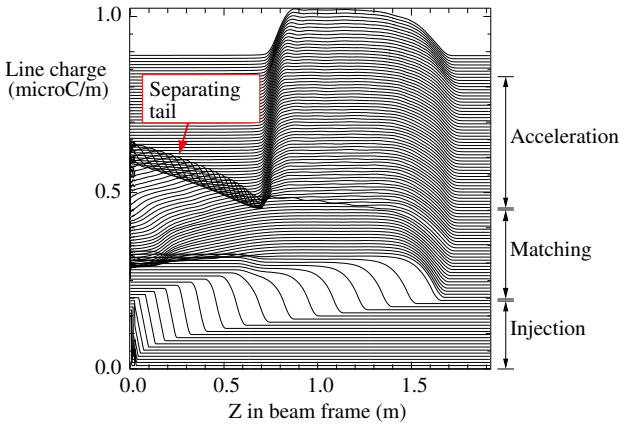

Figure 8: Overlays of the line-charge in the beam frame. Each line shows the line-charge at a particular time as a function of longitudinal position Z in the beam frame. Each curves is shifted up shifted upward in proportion to its time, so that later curves remain visible.

matching section, and other manipulations can be done, with very little perturbation to the beam.

---

[1] D. P. Grote, A, Friedman, I. Haber, and S. S. Yu, "Three-Dimensional Simulations of High-Current Beams in Induction Accelerators with WARP3d," Proceedings of the 1995 International Symposium on Heavy Ion fusion, Fusion Engineering and Design **32-33,** 193-200 (1996).

[2] C. M. Celata, J. W. Kwan, E. P. Lee, M. A. Leitner, B. G. Logan, J-L. Vay, W. L. Waldron, S. S. Yu, J. J. Barnard, R. H. Cohen, A. Friedman, D. P. Grote, A. W. Molvik, W. M. Sharp, D. V. Rose, D. R. Welch, R. C. Davidson, I. D. Kaganovich, H. Qin, and E. A. Startsev, "The Integrated Beam Experiment - a Next Step Experiment for Heavy Ion Fusion," Proc. 3rd Intern. Conf. Inertial Fusion Science Appl., 7-12 September 2003, Monterey, CA (to be published).

[3] J. J. Barnard, L. E. Ahle, F. M. Bieniosek, C. M. Celata, R. C. Davidson, D. P. Grote, E. Henestroza, A. Friedman, J. W. Kwan, B. G. Logan, E. P. Lee, S. M. Lund, W. R. Meier and H. Qin, "Integrated Experiments for Heavy Ion Fusion," *Laser and Particle Beams* **21**, in press (2003).

[4] Peter McCorquodate, *et al.*, "A Node-Centered Local Refinement Algorithm for Poisson's Equation in

Complex Geometries", to be published.

[5] J. L. Vay, *et al.*, "Progress in the Study of Mesh Refinement for Particle-In-Cell Plasma Simulations and it Application to Heavy-Ion Fusion," proceedings of the 2002 International Computational Accelerator Physics conference.